

Autocatalysis for C–H Bond Activation by Ruthenium(II) Complexes in Catalytic Arylation of Functional Arenes

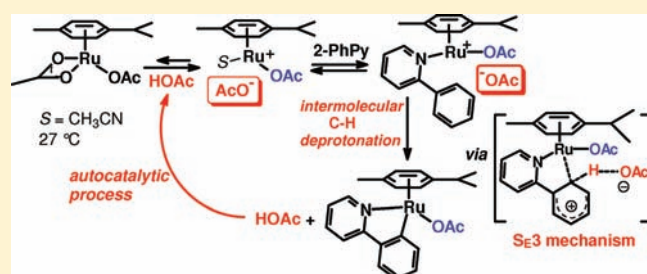
Emmanuel Ferrer Flegeau,[†] Christian Bruneau,[‡] Pierre H. Dixneuf,^{*,‡} and Anny Jutand^{*,†}

[†]Ecole Normale Supérieure, Département de Chimie, UMR CNRS-ENS-UPMC 8640, 24 Rue Lhomond, 75231 Paris Cedex 5, France

[‡]Institut Sciences Chimiques, UMR 6226 CNRS-Université de Rennes, Campus Beaulieu, Université de Rennes, 35042 Rennes, France

S Supporting Information

ABSTRACT: Kinetic data for the C–H bond activation of 2-phenylpyridine by Ru^{II}(carboxylate)₂(*p*-cymene) **I** (acetate) and **I'** (pivalate) are available for the first time. They reveal an irreversible autocatalytic process catalyzed by the coproduct HOAc or HOPiv (acetonitrile, 27 °C). The overall reaction is indeed accelerated by the carboxylic acid coproduct and water. It is retarded by a base, in agreement with an autocatalytic process induced by HOAc or HOPiv that favors the dissociation of one carboxylate ligand from **I** and **I'** and consequently the ensuing complexation of 2-phenylpyridine (2-PhPy). The C–H bond activation initially delivers Ru(O₂CR)(*o*-C₆H₄-Py)(*p*-cymene) **A** or **A'**, containing one carboxylate ligand (OAc or OPiv, respectively). The overall reaction is accelerated by added acetates. Consequently, C–H bond activation (faster for acetate **I** than for pivalate **I'**) proceeds via an intermolecular deprotonation of the C–H bond of the ligated 2-PhPy by the acetate or pivalate anion released from **I** or **I'**, respectively. The 18e complexes **A** and **A'** easily dissociate, by displacement of the carboxylate by the solvent (also favored by the carboxylic acid), to give the same cationic complex **B**⁺ {[Ru(*o*-C₆H₄-Py)(*p*-cymene)(MeCN)]⁺}. Complex **B**⁺ is reactive toward oxidative addition of phenyl iodide, leading to the diphenylated 2-pyridylbenzene.



INTRODUCTION

The catalytic C–C bond formation reaction starting from inert C–H bonds is an attractive challenge, especially for catalysis and more efficient organic syntheses, but also for the selective building of molecular and macromolecular materials. The C–H bond activation/functionalization performed under mild conditions is expected to improve the atom and energy economy of synthetic processes and contribute to the shortening of multiple-step syntheses. Significant achievements in this direction have already been realized by a variety of metal catalysts,¹ and several types of C–H bond activation/functionalization reactions were discovered in the past decade,² including reactions promoted by ruthenium(II) catalysts.^{3,4} A major problem in C–H bond functionalization concerns the regioselectivity of C–H bond cleavage in molecules containing several C–H bonds. It is generally solved by the introduction of a coordinating functional group that directs the formation of a cyclometalated intermediate.¹ The mechanism of C–H bond activation has been discussed.^{1,4a,5–7} Assistance of a ligand or base via an intermolecular⁶ or intramolecular process^{4a,5,7} is generally proposed. Mechanistic studies mainly performed on neutral complexes gave evidence of the assistance of a coordinated ligand (such as carboxylate,^{7a–e} carbonate^{7f} in Pd^{II} catalysts, or carbonate in Ru^{II} catalysts^{4a}) for an intramolecular C–H bond deprotonation in an internal electrophilic substitution or via an agostic M(C–H) bond. Density functional theory (DFT)

calculations established that the initial ligand-assisted C–H bond deprotonation step is a fast process, followed by the slower oxidative addition and reductive elimination.^{4a,5a–c} The catalytic C–H bond functionalization by ruthenium(II) species is currently under successful development,^{3,4} and the influence of carboxylate (mesitylcarboxylate,^{3i,l–n} acetate,^{4a–c} or pivalate^{4c,d}) promoting the activity of ruthenium(II) species has been established. Reactions with Ru^{II} carboxylate catalysts can be performed even in water.^{4d} The strong development of ruthenium(II) catalysts in this field motivates experimental investigations to elucidate the mechanism of C–H bond activation by ruthenium(II) species. Few kinetic data are available in the literature about C–H bond activation by transition metals: pioneering work on palladium(II) complexes by Ryabov et al.^{7b,c} and a recent work by Jones et al.^{5h} on rhodium(III) complexes. To the best of our knowledge, no kinetic data for C–H bond activation by ruthenium are yet available. This prompted us to investigate the kinetics of C–H bond activation by carboxylate–ruthenium(II) complexes,^{4b–d} which significantly promote C–H bond activation, to gain mechanistic insight into this process. 2-Phenylpyridine was selected as a model molecule as it easily gives cyclometalated products with Ru^{II} complexes⁸ and leads to Ru^{II}-catalyzed mono- and diarylation with aryl halides.^{3,4}

Received: March 1, 2011

Published: May 23, 2011

Scheme 1

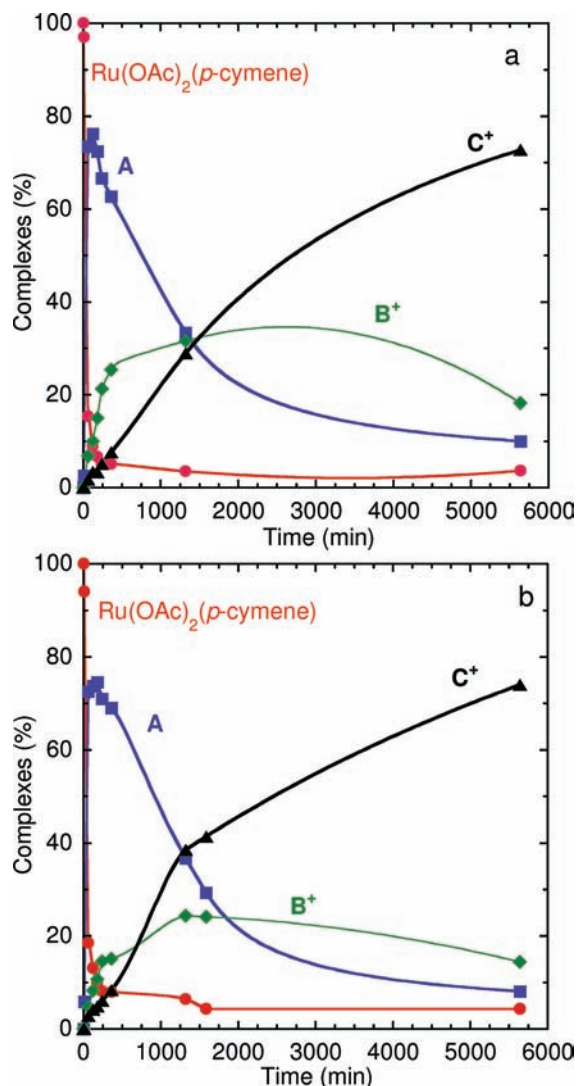
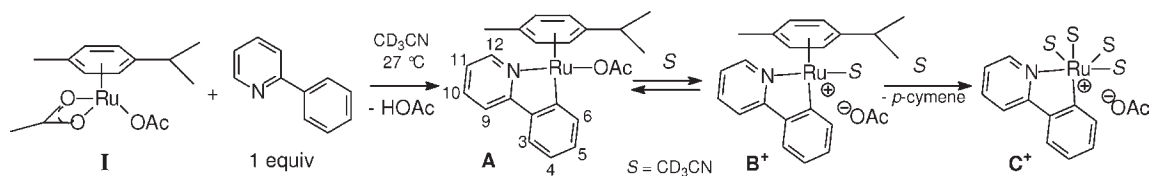


Figure 1. Kinetics of C–H bond activation of 2-PhPy (0.16 M) by Ru(OAc)₂(*p*-cymene) I (0.16 M) in CD₃CN at 27 °C, as monitored by ¹H NMR. (a) Decay of I with time (circles) and formation of complexes A (squares), B⁺ (diamonds), and C⁺ (triangles). (b) Same conditions as in panel a but in the presence of KOAc (3 equiv) added before introduction of 2-PhPy.

We report herein a kinetic study of C–H bond activation of 2-phenylpyridine by Ru(carboxylate)₂(arene) complexes (the carboxylate being acetate or pivalate) in acetonitrile. A surprising unprecedented autocatalytic process was found to take place at 27 °C, catalyzed by the carboxylic acid coproduct. The reaction is indeed greatly accelerated by acetic or pivalic acid and water. The C–H bond deprotonation is irreversible at room temperature.

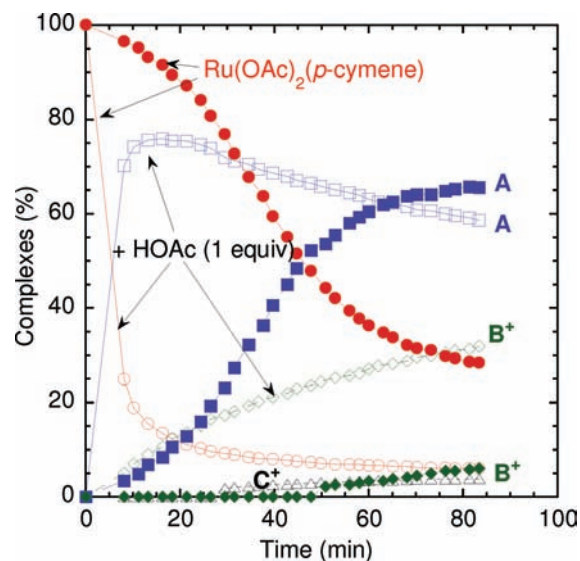


Figure 2. Kinetics of C–H bond activation of 2-PhPy (0.16 M) by Ru(OAc)₂(*p*-cymene) I (0.16 M) in CD₃CN at 27 °C, as monitored by ¹H NMR. Decay of Ru(OAc)₂(*p*-cymene) with time (filled circles) and formation of complexes A (filled squares) and B⁺ (filled diamonds). In the presence of HOAc (1 equiv) added before 2-PhPy, as indicated by the arrows: (empty circles) decay of I and formation of A (empty squares), B⁺ (empty diamonds), and C⁺ (triangles).

The accelerating effect of carboxylates let us propose an intermolecular deprotonation by the carboxylate ion released from Ru^{II}(carboxylate)₂(arene) complexes. In addition, the active species that undergoes oxidative addition to PhI has been characterized.

RESULTS AND DISCUSSION

Kinetics of the Reaction of Ru(OAc)₂(*p*-cymene) with 2-Phenylpyridine. Ru(OAc)₂(*p*-cymene) was first studied because it is a better catalyst for diarylation of 2-phenylpyridine than [RuCl₂(*p*-cymene)]₂.^{4b–d} The reaction of Ru(OAc)₂(*p*-cymene) (I) (0.16 M) with 2-phenylpyridine (2-PhPy) (0.16 M) (i.e., under stoichiometric conditions) was performed in CD₃CN and followed by ¹H NMR spectroscopy at 27 °C. Analysis of the ¹H NMR spectra recorded with time (see the NMR spectra obtained after 266 and 1320 min in Figure S9 of the Supporting Information) revealed that three cyclometalated Ru^{II} complexes were formed [A, B⁺, and C⁺ (Scheme 1)] whose evolution with time is represented in Figure 1a.

The reactivity of I was followed via the decay with time of the doublet [CH(CH₃)₂] of its *p*-cymene ligand at 1.33 ppm (Figures S1 and S9 of the Supporting Information). Meanwhile, a new cyclometalated complex A, RuOAc(*o*-C₆H₄-Py)(*p*-cymene) (Scheme 1), appeared over time, as evidenced by two new close

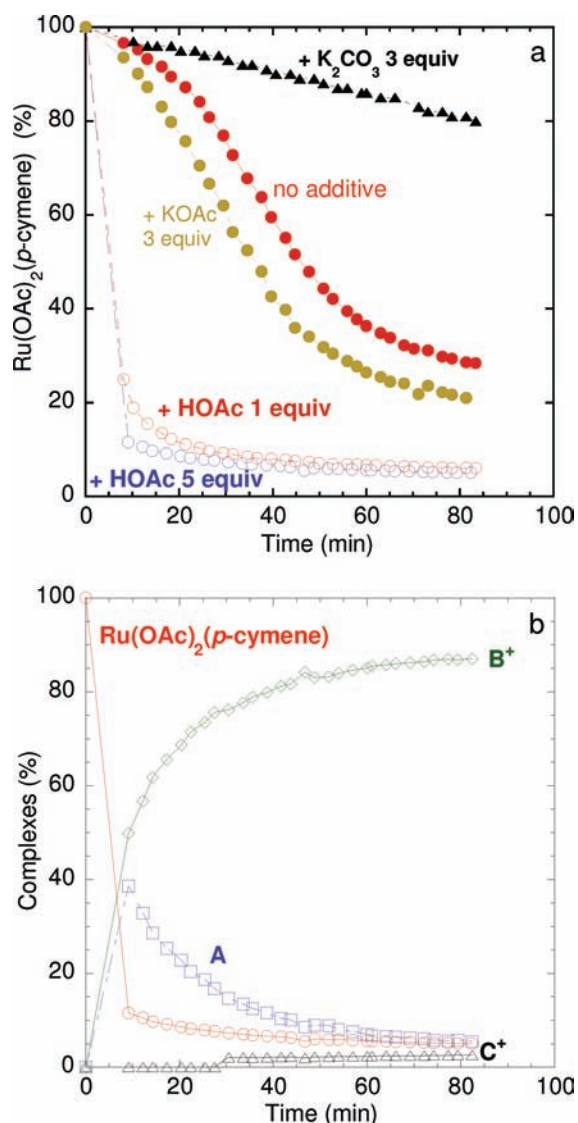
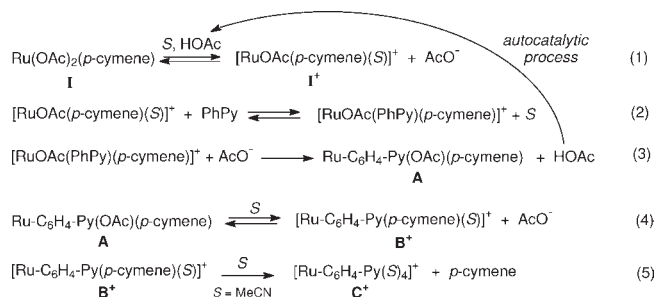


Figure 3. Kinetics of the C–H bond activation of 2-PhPy (0.16 M) by $\text{Ru}(\text{OAc})_2(p\text{-cymene})$ **I** (0.16 M) in CD_3CN at 27 °C, as monitored by ^1H NMR. (a) Decay of **I** with time: alone (filled red circles) or in the presence of 3 equiv of K_2CO_3 (triangles), 3 equiv of KOAc (brown circles), 1 equiv of HOAc (empty red circles), or 5 equiv of HOAc (blue circles). (b) Evolution of **I** (circles), **A** (squares), **B**⁺ (diamonds), and **C**⁺ (triangles) in the reaction of Ph-Py (0.16 M) with **I** (0.16 M) performed in the presence of HOAc (5 equiv).

doublets at 0.85 and 0.83 ppm characteristic of two nonequivalent CH_3 groups [$\text{CH}(\text{CH}_3)_2$] in its *p*-cymene ligand, as well as a doublet at 9.59 ppm characteristic of a proton H_{12} located in an α position relative to the nitrogen in a σ -ligated 2- C_6H_4 -Py group (Figures S2a,b and S9 of the Supporting Information). Importantly, complex **A** contained one acetate ligand (*s*, 1.51 ppm) (Figures S2a,b and S9 of the Supporting Information). The ^1H NMR spectrum of complex **A**, $\text{Ru}(\text{OAc})(o\text{-C}_6\text{H}_4\text{-Py})(p\text{-cymene})$, generated as described above in CD_3CN (Figure S2a,b of the Supporting Information), was compared to that of the same complex **A** generated by reacting the reported^{8b} relevant chloride complex $\text{RuCl}(o\text{-C}_6\text{H}_4\text{-Py})(p\text{-cymene})$ (**D**) with AgOAc in CDCl_3 (vide infra Scheme 4 and Figure S2c,d of the Supporting Information).

Scheme 2



The evolution of **A** with time followed by ^1H NMR revealed that such a complex was not stable [bell-shaped curve (Figure 1a)]. Complex **A** gave a new complex (Figure S9 of the Supporting Information) that was assigned to the cationic complex **B**⁺, OAc^- (Scheme 1) by comparison to an authentic sample of **B**⁺, PF_6^- , independently synthesized in 90% yield (Figures S3 and S4 of the Supporting Information).^{9a} The evolution of **B**⁺ with time also exhibited a maximum (Figure 1a). **B**⁺ was gradually transformed into the cationic species **C**⁺ (Scheme 1)^{9b} in which the *p*-cymene ligand has been replaced with acetonitrile ligands, as shown by the detection of the ^1H NMR protons of the free *p*-cymene (**C**⁺) (Figure S9 of the Supporting Information). Complex **C**⁺ and free *p*-cymene were generated at the same rate from complex **B**⁺. Consequently, the evolution with time of the integration of the doublet [$\text{CH}(\text{CH}_3)_2$] of the free *p*-cymene **C**⁺ at 1.23 ppm characterized the kinetics of formation of **C**⁺ from **B**⁺.

Therefore, the plot of the integration of the respective doublets of $\text{CH}(\text{CH}_3)_2$ for **I**, **A**, **B**⁺, and free *p*-cymene (**C**⁺) (i.e., complex **C**⁺) versus time characterized the kinetics of formation of **A** during C–H bond activation, followed by its evolution toward **B**⁺ and **C**⁺ (Figure 1a). The same complexes **A**, **B**⁺, and **C**⁺ were obtained in the reaction of **I** with 2-PhPy performed in the presence of acetate (introduced as KOAc, 3 equiv) (Figure 1b). However, complex **A** was more stable with time (the maximum of **A** in Figure 1a was sharper than the maximum of **A** in Figure 1b), evidence that the **A** → **B**⁺ + AcO^- reaction was reversible (Scheme 1).

These experiments establish that the *ortho* C–H bond activation of 2-PhPy by complex **I** occurs in <100 min ($t_{1/2} \sim 46$ min) under stoichiometric conditions (0.16 M), in acetonitrile at 27 °C, affording complex **A**, which loses its acetate ligand in a reversible reaction to form **B**⁺, which in turn loses its *p*-cymene ligand to give complex **C**⁺ with longer times (Scheme 1).

The kinetics were then investigated at short times (<100 min) to gain accurate kinetic data for the rate of disappearance of **I** in the C–H bond activation of 2-PhPy, using anisole as an internal standard for the integration of the ^1H NMR signals (vide supra). Surprisingly, the decay of **I** with time was not hyperbolic as expected for a reaction performed under stoichiometric conditions but characterized an autocatalytic process (Figure 2, filled symbols), in which the reaction is accelerated by a product formed in the reaction. Such a mechanism is quite rare in organometallic chemistry. Hartwig has nevertheless reported an autocatalytic process for the oxidative addition of PhBr to $\text{Pd}^0(\text{P}^t\text{Bu}_3)_2$.¹⁰ Because one of the two products formed during C–H bond activation is acetic acid (Scheme 1) detected in the ^1H NMR spectra (Figure S2a of the Supporting Information), its effect on the rate of the reaction was evaluated. Gratifyingly, the **I** → **A** reaction was considerably accelerated: from a $t_{1/2}$ of 45 min in the absence of HOAc to a $t_{1/2}$ of ~ 5 min when performed in the

presence of 1 equiv of acetic acid (Figure 2, empty symbols, data at very short times, $t < 8$ min, are not available because of the NMR shim). The dissociation of acetate ion from **A** to give the cationic complex **B**⁺ was again observed and tremendously amplified (Figure 2, empty symbols). **C**⁺ was also formed in small amounts. Consequently, the overall reaction in which C–H bond activation takes place was favored in the presence of acetic acid, a coproduct responsible for the autocatalytic process. A drastic retarding effect of a base, such as K₂CO₃ (3 equiv) often used in C–H bond functionalizations,^{3,4} was also observed (Figure 3a and Figure S10 of the Supporting Information). It is consistent with the autocatalytic process, as K₂CO₃ neutralized the profitable HOAc acid. The decelerating effect of K₂CO₃ will be discussed below.

Because the reaction is catalyzed by acetic acid, water should accelerate the kinetics by increasing the acidity of acetic acid. The reaction was indeed much faster in the presence of water (10 equiv). Complex **A** was formed in 68 and 77% yields after 8 and 13 min, respectively. The autocatalytic process was also observed in the presence of acetate ions introduced as KOAc (3 equiv), but the reaction became faster than in the absence of added acetates (Figure 3a and Figure S11 of the Supporting Information), which indicates that noncoordinated acetates are involved in a rate-determining step. This accelerating effect of acetate will be discussed below.

Therefore, HOAc formed as a coproduct accelerates C–H bond activation in an autocatalytic process. The 18e complex **I** is expected to first dissociate (eq 1, Scheme 2) to the cationic complex [Ru(OAc)(*p*-cymene)(MeCN)]⁺ (**I**⁺) able to coordinate 2-PhPy via the N atom (eq 2). Such a predissociation to allow complexation of the substrate was also established by Jones et al. in the cyclometalation of aromatic imine by Cp^{*}Rh(OAc)₂.^{5h} The catalytic effect observed in Figure 2 suggests that HOAc is involved in eq 1 by causing a shift of the equilibrium toward its right-hand side. In other words, HOAc favors the dissociation of complex **I** toward the formation of [Ru(OAc)(*p*-cymene)(MeCN)]⁺ (**I**⁺) by acido-basic reaction of the acetate with the protons introduced by HOAc. Indeed, the ¹H NMR spectrum of **I** was modified by addition of HOAc. The singlet of the Me group of the acetate ligands in complex **I** at 1.79 ppm disappeared after addition of HOAc [$n = 10$ equiv (Figure S12a of the Supporting Information)] to give a unique signal common with those of the Me protons of HOAc at 2.00 ppm, evidencing an equilibrium between all ligated and free acetate groups. More interestingly, two new doublets for the aromatic protons of the ligated *p*-cymene were detected at lower field (5.97 and 5.75 ppm) in the presence of HOAc, instead of at 5.87 and 5.63 ppm, respectively, for **I** (Figure S12a of the Supporting Information). Their intensity increased at the expense of those of the initial **I** when the amount of added HOAc was increased [$n = 25$ equiv (Figure S12b of the Supporting Information)], indicative of an equilibrium. Those signals characterize the cationic complex [Ru(OAc)(*p*-cymene)(MeCN)]⁺ (**I**⁺) (eq 1).¹¹ A related effect has also been observed in the presence of trifluoroacetic acid.¹² The dissociation of complex **I** (eq 1) was also favored in the presence of H₂O (Figure S12c of the Supporting Information).

The mechanism leading to C–H activation and ensuing reactions is given in Scheme 2. Once 2-PhPy is ligated to the Ru^{II} center, the C–H bond activation takes place.¹³ Because this reaction first delivered complex **A** with one acetate coordinated to the Ru^{II} center, this suggests that the free acetate released in eq 1 played a key role in the C–H bond activation process by an intermolecular deprotonation, which may be related to an S_E3

mechanism¹⁴ (Scheme 3, eq 6). An intramolecular C–H bond deprotonation in [RuOAc(PhPy)(*p*-cymene)]⁺ by the ligated acetate would have directly generated the cationic complex **B**⁺, which was not observed experimentally, **A** being the first formed product of the reaction (vide supra). Moreover, the accelerating effect of added acetate indicates that noncoordinated acetates are involved in the rate-determining step. The intrinsic rate of an intramolecular process would not be affected by the concentration of acetate {the intramolecular deprotonation in [RuOAc(PhPy)(*p*-cymene)]⁺ would be a zero-order reaction}. However, the concentration of [RuOAc(PhPy)(*p*-cymene)]⁺ should decrease in the presence of acetate because the concentration of [RuOAc(*p*-cymene)(S)]⁺ decreases because of a shift in the equilibrium in eq 1 toward its left-hand side in the presence of excess acetate. Consequently, the overall reaction involving an intramolecular C–H bond activation should be slower in the presence of acetate, as observed with Rh^{III} complexes.^{5h} In contrast, an accelerating effect was observed in the presence of added acetate (Figure 3a), which means that external acetates are involved in the rate-determining deprotonation step, which is thus intermolecular. Under our experimental conditions, the antagonist effect between an accelerating effect in eq 3 and a decelerating effect due to the shift of the equilibrium in eq 1 toward its left-hand side finally favored the accelerating effect. The accelerating effect observed in the presence of added acetate (Figure 3a) supports a three-center electrophilic mechanism analogous to an intermolecular S_E3 mechanism¹⁴ (eqs 3 and 6). The stronger basicity of an external free acetate must compensate for the high local concentration (intramolecular process) but lower basicity of a ligated acetate.^{5a} An alternative mechanism involving an intermolecular mechanism based on an agostic Ru(C–H) bond^{4a} cannot be fully excluded (Scheme 3, eq 7), though the proton of the electrophilic S_E3 intermediate is expected to be more acidic than the agostic H. This intermolecular mechanism contrasts with most DFT calculations (however, all based on neutral complexes) that predict an intramolecular deprotonation by a ligated acetate.¹⁵

C–H bond activation takes place in eq 3, after two successive equilibria (eqs 1 and 2) that affect the kinetics of the overall reaction. Indeed, the disappearance of **I** is accelerated (i) by HOAc interfering in eq 1, (ii) by an increasing concentration of 2-PhPy involved in eq 2 [compare the faster reaction performed in the presence of 3.64 equiv of 2-PhPy to that performed in the presence of 1 equiv of Ph-Py (panels a and c of Figure S17 of the Supporting Information, respectively)], and (iii) by added acetates interfering in eq 3 (“first-order” reaction for external acetates), in agreement with the mechanism proposed in eqs 1–3. The dissociation of **I** to give [Ru(OAc)(*p*-cymene)(S)]⁺ (**I**⁺) is crucial because it allows coordination of 2-PhPy and further C–H bond activation. The formation of **I**⁺ is favored by HOAc and consequently inhibited by K₂CO₃, which neutralized the profitable HOAc. This explained the decelerating effect observed in the presence of K₂CO₃ (Figure 3a).

The rate of the overall C–H bond activation was not significantly sensitive to the solvent provided it was polar. Indeed, close kinetic curves were obtained for the decay of **I** and formation of **A** when the reaction was performed in CD₃CN or in a CD₃CN/CDCl₃ mixture (7:3) (Figure S14 of the Supporting Information). The reaction was, however, considerably slower in toluene, an apolar solvent. Complex **A** was indeed detected in 5 and 46% yield after 27 and 49 h, respectively (27 °C), confirming the hypothesis that complex **I** should

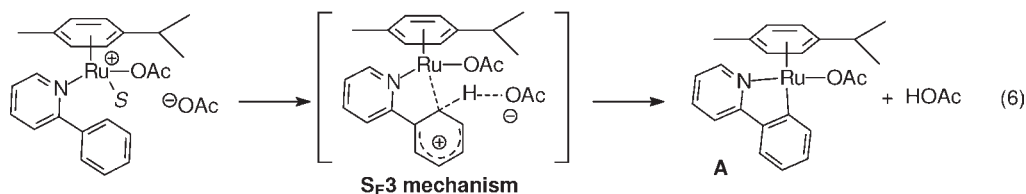
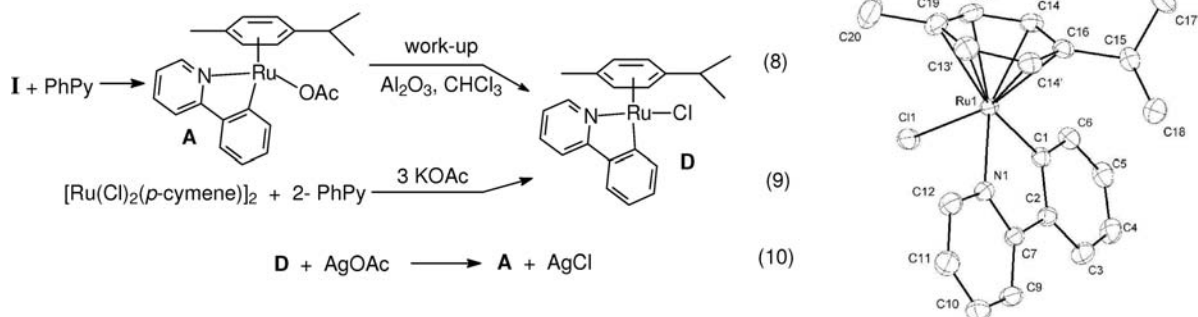
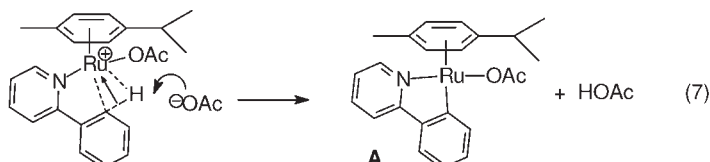
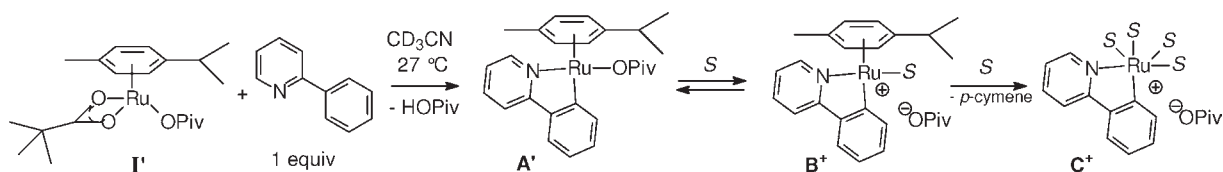
Scheme 3. Deprotonation Mechanism of the *ortho*-C–H Bond of the Ligated 2-PhPy (S = MeCN)Intermolecular mechanism from kinetic data via S_E3 mechanismAlternative intermolecular mechanism involving an agostic *ortho*-C--H--Ru bond

Figure 4. Synthesis and single-crystal X-ray structure of complex D.

Scheme 4



dissociate before reacting with 2-PhPy (eq 1, Scheme 2). Complexes **A** and **B**⁺ and acetate are in equilibrium (eq 4 in Scheme 2). The **B**⁺:**A** ratio was not constant all along the reaction and depended on the reaction conditions. It increased with time because the concentration of released HOAc in the reaction mixture increased as the reaction proceeded. The formation of **B**⁺ from **A** was favored in the presence of increasing amounts of added HOAc (compare Figures 2 and 3b), in agreement with the proposed equilibrium in eq 4.

A relevant complex to **A** but ligated by mesitylcarboxylate as the carboxylate ligand has been isolated by Ackermann et al.³ⁿ after reaction of Ru(O₂CMe)₂(*p*-cymene) with *p*-MeO-PhPy in the presence of K₂CO₃, in toluene. Our attempts to isolate pure complex **A** starting from **I** failed (eq 8). Instead, complex **D** was isolated with Cl as the ligand (Figure 4) formed from **A** during the workup [chromatography on alumina with eluting chlorinated solvents (see the Supporting Information)]. An authentic sample of **D** was obtained by reacting [RuCl₂(*p*-cymene)]₂ with

2-PhPy in the presence of KOAc and characterized by X-ray (eq 9, Figures S7 and S8 of the Supporting Information), showing that Cl is a better ligand for the Ru^{II} center than OAc. Complex **D** was previously reported by Pfeffer et al.^{8b} and was generated in a transmetalation of [RuCl₂(*p*-cymene)]₂ by the organomercurous derivative 2-Py-C₆H₄-HgCl because the direct reaction of [RuCl₂(*p*-cymene)]₂ with 2-PhPy failed.^{8b} Our new procedure for synthesizing complex **D** (eq 9) confirms the beneficial role of acetate in C–H bond activation observed above and in catalytic reactions.^{3m,4b–4d} With complex **D** in hand, the synthesis of complex **A** was achieved by reaction of **D** with AgOAc (eq 10). The ¹H NMR spectrum of the resulting complex **A** in CDCl₃ was then very similar to that of complex **A** generated in situ from **I** in CD₃CN (compare Figures S2a,b and S2c,d of the Supporting Information).¹⁶

Kinetics of the Reaction of Ru(OPiv)₂(*p*-cymene) with 2-Phenylpyridine. The kinetics of the reaction of Ru(O₂C^tBu)₂(*p*-cymene) **I'** (0.16 M) with 2-PhPy (1 equiv) was similarly

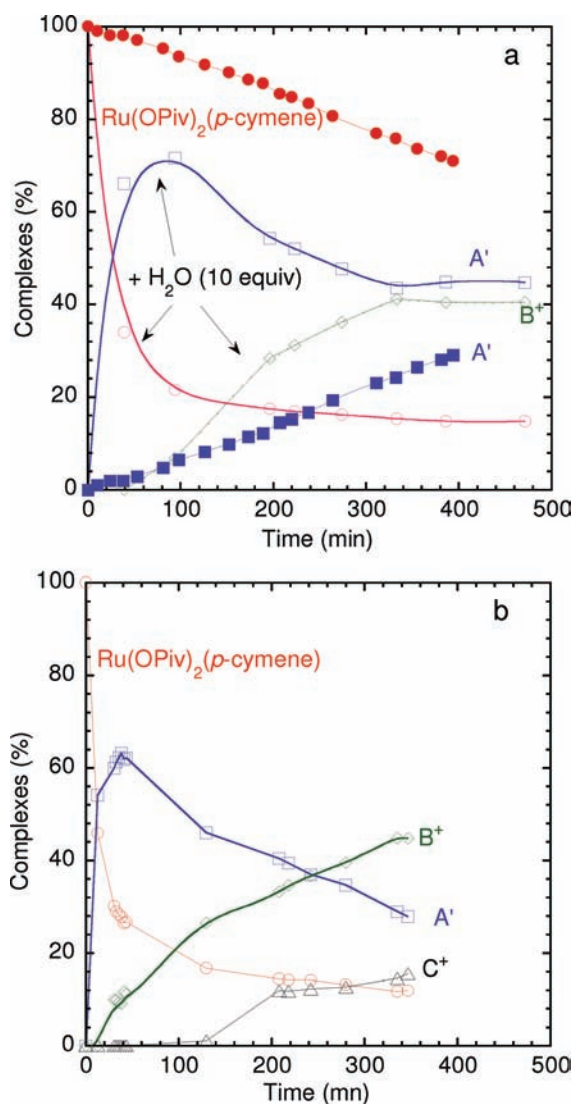
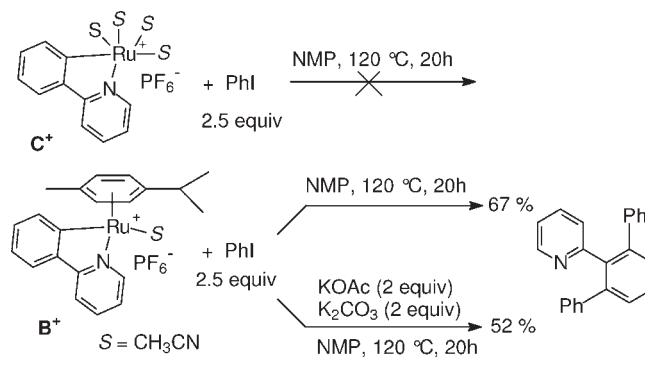


Figure 5. Kinetics of the C–H bond activation of 2-PhPy (0.16 M) by $\text{Ru}(\text{OPiv})_2(p\text{-cymene})$ I' (0.16 M) in a $\text{CD}_3\text{CN}/\text{CDCl}_3$ mixture (350 and 150 μL , respectively) at 27 °C, as monitored by ^1H NMR. (a) Decay of I' with time (filled red circles) and formation of complex A' (filled blue squares). Reaction performed in the presence of H_2O (10 equiv) as indicated by the arrows: (empty red circles) decay of I' with time and formation of complexes A' (empty blue squares) and B⁺ (diamonds). (b) Reaction performed in the presence of HOPiv (5 equiv). See Figure S19 of the Supporting Information for the reaction performed in the presence of 50 equiv of HOPiv.

investigated by ^1H NMR performed in a mixture of CDCl_3 (150 μL) and CD_3CN (350 μL) because of the insolubility of I' in pure acetonitrile. The C–H bond activation led to the formation of complex A' (Scheme 4) with OPiv as a σ -ligand (s, 0.45 ppm) (Figures S16 and S17a of the Supporting Information). The relative amount of the two complexes, I' and A' (filled symbols in Figure 5a), was estimated by the respective integration of the CH_3 of the *p*-cymene ligand of I' (2.13 ppm) and A' (1.78 ppm) (Figure S16 of the Supporting Information).¹⁷ The formation of HOPiv was also observed in the ^1H NMR spectra (Figures S16 and S17a of the Supporting Information).

The reaction of I' with 2-PhPy ($t_{1/2} \gg 400$ min) was much slower than that of I ($t_{1/2} = 46$ min) (Figure S18 of the Supporting

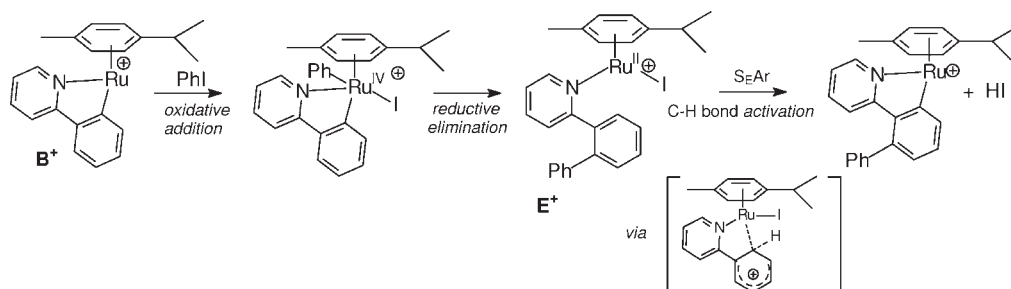
Scheme 5



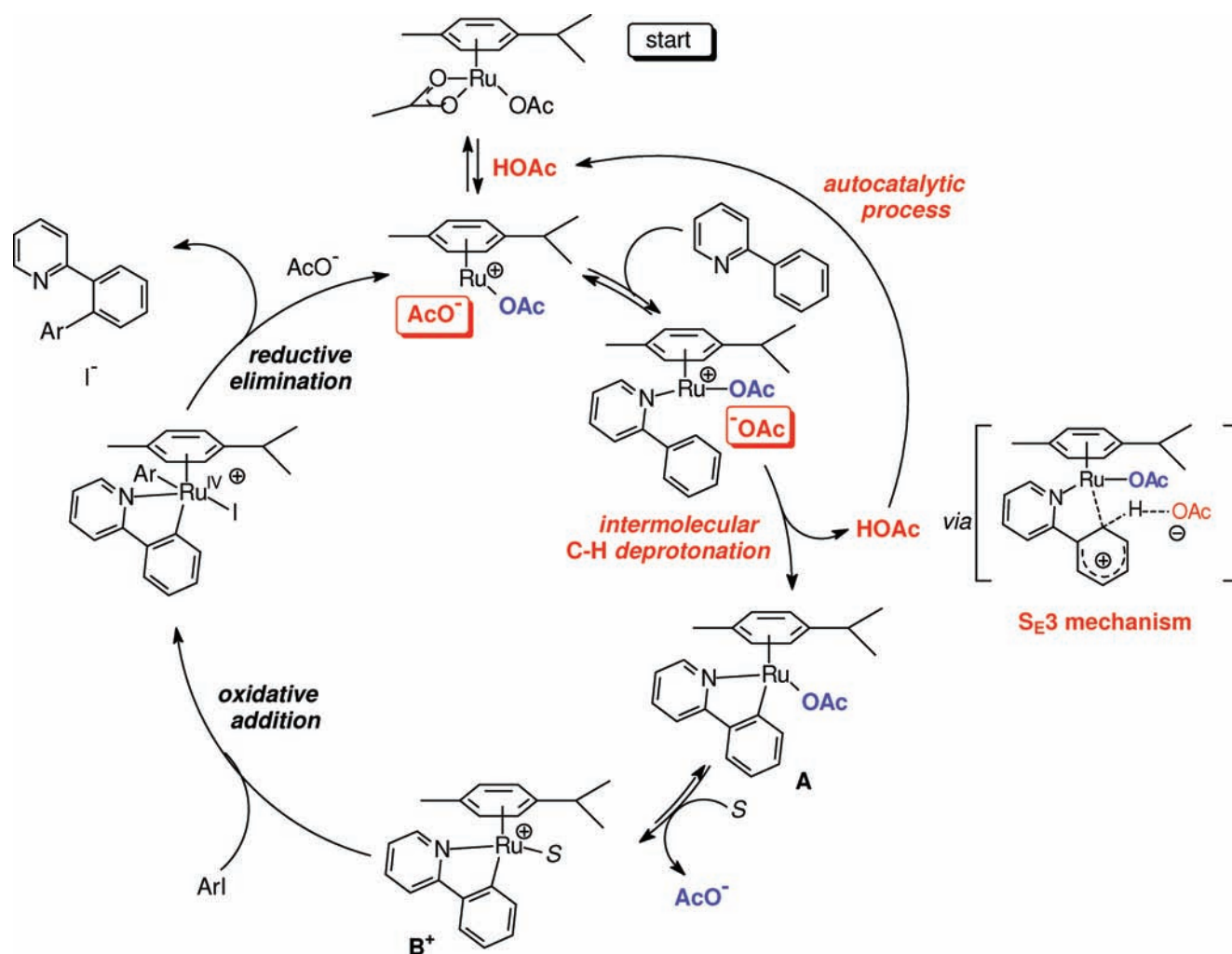
Information) when performed in the same $\text{CD}_3\text{CN}/\text{CDCl}_3$ solvent mixture (7:3) with the same initial concentrations. It was also considerably accelerated in the presence of HOPiv [5 equiv; $t_{1/2} \sim 13$ min (Figure 5b)], consistent with an autocatalytic process, which is observed for I.

The effect of HOPiv on the dissociation of PivO^- from I' was studied. No significant dissociation was observed even in the presence of 50 equiv of HOPiv, suggesting that PivO^- is a better ligand in I' than AcO^- in I. Even if PivO^- is more basic than AcO^- , the overall reaction is slower because at identical concentrations of I' and I, the available concentration of $[\text{Ru}(\text{OPiv})(p\text{-cymene})(\text{S})]^+$ is lower than that of $[\text{Ru}(\text{OAc})(p\text{-cymene})(\text{S})]^+$ in their respective equilibria with the neutral I' and I. As for complex I, the reaction was much faster in the presence of water (10 equiv), which increased the acidity of the pivalic acid and favored the dissociation of I' ($t_{1/2} \sim 30$ min) (Figure 5a, empty symbols).¹⁸ The formation of complex A' as the first product of C–H bond activation favors an intermolecular deprotonation. The intermolecular deprotonation from I' is slower than that performed from I because of the lower concentration of the released PivO^- compared to that of AcO^- in their respective equilibria with I' and I. Complex A' was also found to be in equilibrium with B⁺. The B⁺:A' ratio increased when the concentration of the added HOPiv increased (compare Figure 4 and Figure S19 of the Supporting Information). B⁺ also lost its *p*-cymene ligand (C') to deliver C⁺ at longer times (Scheme 4 and Figure S17c of the Supporting Information). The mechanisms established for the activation of the C–H bond of 2-PhPy by I or I' are thus very similar (Schemes 2 and 3).

Irreversible C–H Bond Activation. Complex I (0.16 M) was reacted with 2-PhPy (2 equiv) in CD_3CN in the presence of D_2O (10 equiv). The reaction was quite fast, taking place within 8 min in agreement with the water accelerating effect observed above and with the increased concentration of 2-PhPy, as well. The first recorded ^1H NMR spectrum revealed the formation of complex A with unreacted 2-PhPy in an almost stoichiometric amount (Figure S20 of the Supporting Information). The five protons of the Ph group of unreacted 2-PhPy [a doublet integrating for 2 H at 8.05 ppm and a multiplet integrating for 3 H at 7.5 ppm (see Figure S20b of the Supporting Information)] were identical to those of the initial 2-PhPy, ruling out any incorporation of deuterium into the Ph group of 2-PhPy at 27 °C at the RMN accuracy. The proton of acetic acid formed during C–H bond activation must rapidly exchange with the D of D_2O leading to DOAc. Because there is no incorporation of the deuterium atom into 2-PhPy, this suggests that C–H bond activation did not exhibit any reversibility under our experimental conditions (acetonitrile

Scheme 6. Mechanism of the Stoichiometric Monophenylation and Second C–H Bond Activation in the Absence of Acetate Ions^a

^a The solvents of all cationic Ru^{II} complexes have been omitted for the sake of clarity, in addition to the counteranion of all PF₆[−] complexes.

Scheme 7. Mechanism for the Monoarylation of 2-Phenylpyridine Catalyzed by Ru(OAc)₂(*p*-cymene)^a

^a The solvent of the cationic complexes ligated by one acetate has been omitted for the sake of clarity.

at 27 °C). No D incorporation was observed in the presence of a larger amount of D₂O (40 equiv) at room temperature.¹⁹ In a recent work by Jones et al.,^{5h} the reaction of Cp*Rh(OAc)₂ with an aromatic imine (Ar-imine) was found to be reversible in the presence of DOAc.^{5h} In that case, the observed retarding effect of added acetates indicated that the rate-determining step is the dissociation of Cp*Rh(OAc)₂ to Cp*Rh(OAc)⁺ leading to Cp*Rh(OAc)(Ar-imine)⁺.

An intramolecular deprotonation of the C–H bond by the ligated acetate in the Cp*Rh(OAc)(Ar-imine)⁺ complex took place leading to Cp*Rh(σ -Ar-imine)(HOAc)⁺. The HOAc ligand is then rapidly deprotonated by an external acetate to form Cp*Rh(OAc)(σ -Ar-imine),^{5h} a complex related to **A** in this work. In our case, the irreversibility of C–H bond activation (vide supra) indicates that **B**⁺(HOAc) cannot be formed in an intramolecular reversible

deprotonation (no incorporation of D in the presence of DOAc). The irreversibility of C–H bond activation and the accelerating effect of added acetate revealed in this work reinforce our conclusion about the intermolecular process for the activation of 2-PhPy by the ruthenium complex **I**, leading first to complex **A**. The comparison of Rh^{III}- and Ru^{II}-promoted C–H bond activation shows that the intimate mechanism of the C–H bond deprotonation step strongly depends on the nature of the metal and ligand.

Oxidative Addition following C–H Bond Activation by Deprotonation. All our attempts to observe any oxidative addition of aryl iodides to **I** failed, even at high temperatures (130 °C). Because C–H bond activation was observed at room temperature under stoichiometric conditions ($t_{1/2} = 46$ min when $[I] = [2\text{-PhPy}] = 0.16$ M; $t_{1/2} = 5$ min when $[I] = [2\text{-PhPy}] = [\text{HOAc}] = 0.16$ M), the catalytic cycle proceeds first by C–H bond activation, followed by slower oxidative addition and finally reductive elimination.^{4a} C–H bond activation by complex **I** led first to **A** and then to **B**⁺ and **C**⁺. Complex **C**⁺ did not react with PhI in the absence or presence of a base (Scheme 5). Because of some difficulty in isolating pure complex **A** in dissociating solvents because of the formation of **B**⁺, the reaction of PhI (2.5 equiv) with isolated complex **B**⁺PF₆[−] was studied, first in the absence of any base. After 20 h in NMP at 120 °C, the doubly arylated product was isolated in 67% yield (Scheme 5), showing that a second C–H bond activation/functionalization took place.

The 18e complex **A** generated first in C–H bond activation cannot be reactive in oxidative addition. Consequently, dissociation from **A** to **B**⁺, emphasized by the coproduct HOAc, is required for the oxidative addition to PhI (Scheme 6). This hypothesis was also confirmed by the fact that no reaction with PhI took place from the 18e complex **D**, which could not easily dissociate its chloride to generate the reactive **B**⁺. The second C–H bond activation proceeded in the absence of any base. The reductive elimination from the cationic Ru^{IV} complex generates a cationic Ru^{II} complex **E**⁺ that probably did not release any iodide in solutions (Scheme 6). Only an intramolecular C–H bond activation could take place without the assistance of a base, as in a classical S_EAr mechanism, the Ru^{II} center in complex **E**⁺ being more electrophilic than in [Ru(OAc)(PhPy)(*p*-cymene)(S)]⁺ (Scheme 6).

The same reaction from complex **B**⁺PF₆[−] was performed in the presence of both KOAc and K₂CO₃ (as in catalytic reactions) and delivered the doubly arylated product in 52% yield (Scheme 5). In the presence of acetate, the second C–H bond activation likely proceeds via an S_E3 mechanism as well as proposed in Scheme 3.

A full mechanism is proposed in Scheme 7 for the mono-phenylation of 2-phenylpyridine catalyzed by Ru(OAc)₂(*p*-cymene) based on the kinetic studies described above with identification of two key intermediate Ru^{II} species: complex **A** formed during C–H bond activation by an intermolecular deprotonation of the ligated 2-PhPy by an external acetate ion and complex **B**⁺ active in the oxidative addition to PhI. The kinetics determined in the presence of added acetic acid have revealed a remarkable double role of the carboxylic acid: (i) acceleration of the overall C–H bond activation via the favored dissociation of acetate from Ru(OAc)₂(*p*-cymene) and (ii) acceleration of the dissociation of complex **A** to complex **B**⁺, which plays a key role in oxidative addition. This mechanism is also valid for Ru(OPiv)₂(*p*-cymene) with the same key role of HOPiv.

The C–H bond activation of 2-PhPy was much faster (27 °C) than the following oxidative addition (120 °C) that becomes rate-determining. It appears that an extra base as K₂CO₃ is

required in reactions catalyzed by Ru(OAc)₂(*p*-cymene).^{4b–d} As established in this work, the overall C–H bond activation becomes slower in the presence of K₂CO₃, which quenches the carboxylic acid coproduct at the origin of the fast C–H bond activation. In the presence of K₂CO₃, the rate of C–H bond activation became slower and thus closer to the rate of the following slower oxidative addition, which favors the efficiency of the catalytic reaction by bringing the rate of the two successive reactions closer to each other. Indeed, a catalytic cycle becomes more efficient and productive when the rates of the different steps become close to each other.²⁰

CONCLUSION

It is established from kinetic data, available for the first time for Ru^{II} complexes, that the C–H bond activation of 2-PhPy by Ru(OAc)₂(*p*-cymene) **I** or Ru(OPiv)₂(*p*-cymene) **I'** is an unexpected autocatalytic process, catalyzed by the coproduct of the cyclometalated complex, i.e., HOAc or HOPiv, respectively. The reaction is indeed accelerated by the carboxylic acid and by water that enhances the acidity of the acid coproduct and retarded by a base (e.g., K₂CO₃), in agreement with an autocatalytic process induced by the carboxylic acid coproduct. The reaction is irreversible at room temperature. The carboxylic acid favors the dissociation of one carboxylate ligand from **I** and **I'** and consequently the ensuing complexation of 2-PhPy. The reaction is faster in the presence of added KOAc. C–H bond activation thus appears to proceed via an intermolecular deprotonation of the ligated 2-PhPy by the acetate or pivalate ion, reversibly released from **I** or **I'**, respectively, following the unexpected reactivity order for C–H bond activation: Ru(OAc)₂(*p*-cymene) > Ru(OPiv)₂(*p*-cymene). This inversion of reactivity is due to a stronger coordination of the more basic pivalate to the Ru^{II} center in **I'**, which inhibits (i) the complexation of 2-PhPy and (ii) the intermolecular deprotonation due to the lower concentration of the released PivO[−] compared to AcO[−] in their respective equilibria with **I'** and **I**. In both cases, the reaction gives Ru(O₂CR)(*o*-C₆H₄-Py)(*p*-cymene) ligated by acetate (**A**) or pivalate (**A'**) in equilibrium with the common cationic complex **B**⁺ {[Ru(*o*-C₆H₄-Py)(*p*-cymene)(MeCN)]⁺}. The latter was found to be active in the oxidative addition of PhI to generate the diarylated product.

The autocatalytic C–H bond activation of 2-PhPy accelerated by carboxylic acids observed in this work is likely a general feature. In the more developed palladium-catalyzed C–H bond functionalization, it appears that C–H bond activations were improved by the use of acetic acid^{11,21a–21c} or pivalic acid^{11,21d} as a solvent. Moreover, a recent paper revealed that C–H bond activation of 2-PhPy by Cu(OAc)₂ was accelerated by pivalic acid.^{21e} The generality of the autocatalytic C–H bond activation established in this work is under investigation.

ASSOCIATED CONTENT

S Supporting Information. NMR spectra of complexes **I**, **I'**, **A**, **A'**, **B**⁺PF₆[−], **C**⁺PF₆[−], and **D** and kinetic curves for C–H bond activation of 2-PhPy by **I** or **I'** with the effect of additives and related experimental parts. This material is available free of charge via the Internet at <http://pubs.acs.org>.

AUTHOR INFORMATION

Corresponding Author

anny.jutand@ens.fr

ACKNOWLEDGMENT

Centre National de la Recherche Scientifique (CNRS), Ecole Normale Supérieure (ENS), and ANR-09-BLAN-0101-02 RuCHCAT are thanked for financial support and for a grant to E.F.F. (ANR). We thank two undergraduate students, Géraldine Lam and Rémi Grosjean.

REFERENCES

- (1) For reviews, see: (a) Ryabov, A. D. *Chem. Rev.* **1990**, *90*, 403–424. (b) Miura, M.; Nomura, M. *Current Topics in Chemistry*; Springer-Verlag: Berlin, 2002; Vol. 129, pp 212–241. (c) Kakiuchi, F.; Murai, S. *Acc. Chem. Res.* **2002**, *35*, 826–834. (d) Kakiuchi, F.; Chatani, N. In *Topics in Organometallic Chemistry*; Bruneau, C., Dixneuf, P. H., Eds.; Springer-Verlag: Berlin, 2004; Vol. 11, pp 45–79. (e) Ritleng, V.; Sirlin, C.; Pfeffer, M. *Chem. Rev.* **2002**, *102*, 1731–1770. (f) Campeau, L. C.; Fagnou, K. *Chem. Commun.* **2006**, 1253–1264. (g) Alberico, D.; Scott, M. E.; Lautens, M. *Chem. Rev.* **2007**, *107*, 174–238. (h) Seregin, I. V.; Gevorgyan, V. *Chem. Soc. Rev.* **2007**, *36*, 1173–1193. (i) Lewis, J. C.; Bergman, R. G.; Ellman, J. A. *Acc. Chem. Res.* **2008**, *41*, 1013–1025. (j) Ackermann, L.; Vicente, R.; Kapdi, A. R. *Angew. Chem., Int. Ed.* **2009**, *48*, 9792–9826. (k) Daugulis, O.; Do, H.-Q.; Shabashov, D. *Acc. Chem. Res.* **2009**, *42*, 1074–1086. (l) Lyons, T. W.; Sanford, M. S. *Chem. Rev.* **2010**, *110*, 1147–1139. (m) Colby, D. A.; Bergman, R. G.; Ellman, J. A. *Chem. Rev.* **2010**, *110*, 624–655. (n) Jazzar, R.; Hitce, J.; Renaudat, A.; Sofack-Kreutzer, J.; Baudoin, O. *Chem.—Eur. J.* **2010**, *16*, 2654–2672. (o) Sun, C.-L.; Li, B.-J.; Shi, Z.-J. *Chem. Commun.* **2010**, 46, 677–685. (p) Special Issue on Selective Functionalization of C-H Bonds. *Chem. Rev.* **2010**, *110*, 575–1211. (q) Ackermann, L. *Chem. Rev.* **2011**, *111*, 1314–1345.
- (2) Selected examples of C–H bond activation or functionalization: (a) Zhang, X.; Fried, A.; Knapp, S.; Goldman, A. S. *Chem. Commun.* **2003**, 2060–2061. (b) Chiong, H. A.; Pham, Q. N.; Daugulis, O. *J. Am. Chem. Soc.* **2007**, *129*, 9879–9884. (c) Bolig, A. D.; Brookhart, M. J. *Am. Chem. Soc.* **2007**, *129*, 14544–14545. (d) Campeau, L.-C.; Bertrand-Laperle, M.; Leclerc, J.-P.; Villemure, E.; Gorelsky, S.; Fagnou, K. *J. Am. Chem. Soc.* **2008**, *130*, 3276–3277. (e) Berman, A. M.; Lewis, J. C.; Bergman, R. G.; Ellman, J. A. *J. Am. Chem. Soc.* **2008**, *130*, 14926–14927. (f) Boutadla, O.; Al-Duaij, O.; Davies, D. L.; Griffith, G. A.; Singh, K. *Organometallics* **2009**, *28*, 433–440. (g) Martinez, R.; Simon, M.-O.; Chevalier, R.; Pautigny, C.; Genet, J.-P.; Darses, S. *J. Am. Chem. Soc.* **2009**, *131*, 7887–7895. (h) Jia, Y.-X.; Kündig, E. P. *Angew. Chem., Int. Ed.* **2009**, *48*, 1636–1639. (i) Yoshikai, N.; Matsumoto, A.; Norinder, J.; Nakamura, E. *Angew. Chem., Int. Ed.* **2009**, *48*, 2925–2928. (j) Bernini, R.; Fabrizi, G.; Sferazza, A.; Cacchi, S. *Angew. Chem., Int. Ed.* **2009**, *48*, 8078–8081. (k) Vetter, A. J.; Rieth, R. D.; Brennessel, W. W.; Jones, W. D. *J. Am. Chem. Soc.* **2009**, *131*, 10742–10752. (l) Arnold, P. L.; Sanford, M. S.; Pearson, S. M. *J. Am. Chem. Soc.* **2009**, *131*, 13912–13913. (m) Liegault, B.; Lapointe, D.; Caron, L.; Vlassova, A.; Fagnou, K. *J. Org. Chem.* **2009**, *74*, 1826–1834. (n) Xiao, B.; Fu, J.; Xu, J.; Gong, T. J.; Dai, J. J.; Yi, J.; Liu, L. *J. Am. Chem. Soc.* **2010**, *132*, 468–469. (o) Wasa, M.; Worrell, B. T.; Yu, J. Q. *Angew. Chem., Int. Ed.* **2010**, *49*, 1275–1277. (p) Roger, J.; Pozgan, F.; Doucet, H. *Adv. Synth. Catal.* **2010**, *352*, 696–710. (q) Prokopcova, H.; Bergman, S. D.; Aelvoet, K.; Smout, V.; Herrebout, W.; Van der Veken, B.; Meerpoel, L.; Maes, B. U. W. *Chem.—Eur. J.* **2010**, *16*, 13063–13067. (r) Xi, P.; Yang, F.; Qin, S.; Zhao, D.; Lan, J.; Gao, G.; Hu, C.; You, J. *J. Am. Chem. Soc.* **2010**, *132*, 1822–1824. (s) Shuai, Q.; Yang, L.; Guo, X.; Basle, O.; Li, C.-J. *J. Am. Chem. Soc.* **2010**, *132*, 12212–12213. (t) Chen, Q.; Ilies, L.; Nakamura, E. *J. Am. Chem. Soc.* **2011**, *133*, 428–429.
- (3) For ruthenium(II)-catalyzed functionalization of C–H bonds, see: (a) Oi, S.; Fukita, S.; Hirata, N.; Watanuki, N.; Miyano, S.; Inoue, Y. *Org. Lett.* **2001**, *3*, 2579–2581. (b) Oi, S.; Ogino, Y.; Fukita, S.; Inoue, Y. *Org. Lett.* **2002**, *4*, 1783–1785. (c) Oi, S.; Sakai, K.; Inoue, Y. *Org. Lett.* **2005**, *7*, 4009–4011. (d) Oi, S.; Funayama, R.; Hattori, T.; Inoue, Y. *Tetrahedron* **2008**, *64*, 6051–6059. (e) Oi, S.; Sato, H.; Sugawara, S.; Inoue, Y. *Org. Lett.* **2008**, *10*, 1823–1826. (f) Ackermann, L. *Org. Lett.* **2005**, *7*, 3123–3125. (g) Ackermann, L.; Althammer, A.; Born, R. *Angew. Chem., Int. Ed.* **2006**, *45*, 2619–2622. (h) Ackermann, L.; Born, R.; Alvarez-Bercedo, P. *Angew. Chem., Int. Ed.* **2007**, *46*, 6364–6367. (i) Ackermann, L.; Vicente, R.; Althammer, A. *Org. Lett.* **2008**, *10*, 2299–2302. (j) Ackermann, L.; Mulzer, M. *Org. Lett.* **2008**, *10*, 5043–5045. (k) Ackermann, L.; Althammer, A.; Born, R. *Tetrahedron* **2008**, *64*, 6115–6124. (l) Ackermann, L.; Althammer, A.; Fenner, S. *Angew. Chem., Int. Ed.* **2009**, *48*, 201–204. (m) Ackermann, L.; Novak, P.; Vicente, R.; Hofmann, N. *Angew. Chem., Int. Ed.* **2009**, *48*, 6045–6048. (n) Ackermann, L.; Vicente, R.; Potukuchi, H. K.; Pirovano, V. *Org. Lett.* **2010**, *12*, 5032–5035.
- (4) For ruthenium(II)-catalyzed C–H bond activation/function-alization, see: (a) Özdemiir, I.; Demir, S.; Cetinkaya, B.; Gourlaouen, C.; Maseras, F.; Bruneau, C.; Dixneuf, P. H. *J. Am. Chem. Soc.* **2008**, *130*, 1156–1157. (b) Požgan, F.; Dixneuf, P. H. *Adv. Synth. Catal.* **2009**, *351*, 1737–1743 (presented as poster 200, 23rd ICOMC, Rennes, France, July 2008). (c) Arockiam, P.; Poirier, V.; Fischmeister, C.; Bruneau, C.; Dixneuf, P. H. *Green Chem.* **2009**, *11*, 1871–1875. (d) Arockiam, P.; Fischmeister, C.; Bruneau, C.; Dixneuf, P. H. *Angew. Chem., Int. Ed.* **2010**, *49*, 6629–6632. (e) Deng, G.; Zhao, L.; Li, C.-J. *Angew. Chem., Int. Ed.* **2008**, *47*, 6278–6282. (f) Cheng, K.; Zhang, Y.; Zhao, J.; Xie, C. *Synlett* **2008**, 1325–1330. (g) Cheng, F.; Yao, B.; Zhao, J.; Zhang, Y. *Org. Lett.* **2008**, *10*, 5309–5312. (h) Kochi, T.; Urano, S.; Seki, H.; Mizushima, E.; Sato, M.; Kakiuchi, F. *J. Am. Chem. Soc.* **2009**, *131*, 2792–2793. (i) Guo, X.; Deng, G.; Li, C.-J. *Adv. Synth. Catal.* **2009**, *351*, 2071–2074. (j) Li, H.; Wei, W.; Xu, Y.; Zhang, C.; Wan, X. *Chem. Commun.* **2011**, 47, 1497–1499. (k) Luo, N.; Yu, Z. *Chem.—Eur. J.* **2010**, *16*, 787–791. (l) Prades, A.; Poyatos, M.; Peris, E. *Adv. Synth. Catal.* **2010**, *352*, 1155–1162. (m) Ueyama, T.; Mochida, S.; Fukutani, T.; Hirano, K.; Satoh, T.; Miura, M. *Org. Lett.* **2011**, *13*, 706–708. (n) Ouellet, S. G.; Roy, A.; Molinaro, C.; Angelaud, R.; Marcoux, J. F.; O’Shea, P. D.; Davies, I. W. *J. Org. Chem.* **2011**, *76*, 1436–1439.
- (5) For reviews on mechanisms of C–H bond activation, see refs 1a and 1q and the following: (a) Boutadla, Y.; Davies, D. L.; Macgregor, S. A.; Poblador-Bahamonde, A. I. *Dalton Trans.* **2009**, 5820–5831. (b) Balcells, D.; Clot, E.; Eisenstein, O. *Chem. Rev.* **2010**, *110*, 749–823. (c) Lapointe, D.; Fagnou, K. *Chem. Lett.* **2010**, *39*, 1118–1126. For other metals than Pd and Ru (mainly Ir and Rh), see: (d) Vigalok, A.; Uzan, O.; Shimon, L. J. W.; Ben-David, Y.; Martin, J. M. L.; Milstein, D. *J. Am. Chem. Soc.* **1998**, *120*, 12539–12544. (e) Davies, D. L.; Al-Duaij, O.; Fawcett, J.; Giardiello, M.; Hilton, S. T.; Russell, D. R. *Dalton Trans.* **2003**, 4132–4138. (f) Davies, D. L.; Donald, S. M. A.; Al-Duaij, O.; Macgregor, S. A.; Pölleth, M. *J. Am. Chem. Soc.* **2006**, *128*, 4210–4211. (g) Oxgaard, J.; Tenn, W. J., III; Nielsen, R. J.; Periana, R. A.; Goddard, W. A., III *Organometallics* **2007**, *26*, 1565–1567. (h) Li, L.; Brennessel, W. W.; Jones, W. D. *Organometallics* **2009**, *28*, 3492–3500. (i) Boutadla, Y.; Davies, D. L.; Macgregor, S. A.; Poblador-Bahamonde, A. I. *Dalton Trans.* **2009**, 5887–5893. (j) Tsuruji, H.; Fujita, S.; Choi, G.; Yamagata, T.; Ito, S.; Miyasaka, H.; Mashima, K. *Organometallics* **2010**, *29*, 4120–4129. (k) Davies, D. L.; Macgregor, S. A.; Poblador-Bahamonde, A. I. *Dalton Trans.* **2010**, *39*, 10520–10527.
- (6) For intermolecular deprotonation, see: (a) Garcia-Cuadrado, D.; De Mendoza, P.; Braga, A. A. C.; Maseras, F.; Echevarren, A. M. *J. Am. Chem. Soc.* **2007**, *129*, 6880–6986. (b) Pascual, P.; De Mendoza, P.; Braga, A. A. C.; Maseras, F.; Echevarren, A. M. *Tetrahedron* **2008**, *64*, 6021–6029. (c) For sp³ C–H bond activation, see: Häller, L. J. L.; Page, M. J.; Macgregor, S. A.; Mahon, M. F.; Whittlesey, M. K. *J. Am. Chem. Soc.* **2009**, *131*, 4604–4605.
- (7) For intramolecular base-assisted deprotonation, see: (a) Sokolov, V. I.; Troitskaya, L. L.; Reutov, O. A. *J. Organomet. Chem.* **1979**, *182*, 537–546. (b) Ryabov, A. D.; Sakodinskaya, I. K.; Yatsimirsky J. Chem. Soc., *Dalton Trans.* **1985**, 2629–2638. (c) Kurzev, A. A.; Kazankov, G. M.; Ryabov, A. D. *Inorg. Chim. Acta* **2002**, *340*, 192–196. (d) Davies, D. L.; Donald, S. M. A.; Macgregor, S. A. *J. Am. Chem. Soc.* **2005**, *127*, 13754–13755. (e) LaFrance, M.; Fagnou, K. *J. Am. Chem. Soc.* **2006**, *128*, 16496–16497. (f) Garcia-Cuadrado, D.; Braga, A. A. C.; Maseras, F.; Echevarren, A. M. *J. Am. Chem. Soc.* **2006**, *128*, 1066–1067.
- (8) (a) Fernandez, S.; Pfeffer, M.; Ritleng, V.; Sirlin, C. *Organometallics* **1999**, *18*, 2390–2394. (b) Djukic, J.-P.; Berger, A.; Duquenne, M.;

Pfeffer, M.; de Cian, A.; Kyriakos-Gruber, N.; Vachon, J.; Lacour, J. *Organometallics* **2004**, *23*, 5757–5767. (c) Djukic, J.-P.; Sortais, J.-B.; Barmoy, L.; Pfeffer, M. *Eur. J. Inorg. Chem.* **2009**, *23*, 817–853. (d) Ryabov, A. D.; Sukharev, V. S.; Alexandrova, L.; Le Lagadec, R.; Pfeiffer, M. *Inorg. Chem.* **2001**, *40*, 6528–6532.

(9) (a) The ^1H NMR signals of B^+, OAc^- generated in situ were located slightly downfield with respect to those of isolated $\text{B}^+, \text{PF}_6^-$ due to the change in the counteranion (H_{12} at 9.27 and 9.19 ppm, respectively). (b) Complex C^+ with PF_6^- as the counteranion has been independently synthesized and isolated in 91% yield, using a modified procedure reported previously.^{8a} Its ^1H NMR spectrum was very similar to those observed during the kinetic study (Figure S5 of the Supporting Information). The ^1H NMR signals of C^+, OAc^- generated in situ were located slightly downfield with respect to those of $\text{C}^+, \text{PF}_6^-$ due to the change in the counteranion (H_{12} at 8.96 and 8.91 ppm, respectively).

(10) Barrios-Landeros, F.; Carrow, B. P.; Hartwig, J. F. *J. Am. Chem. Soc.* **2008**, *130*, 5842–5843.

(11) (a) Two different equilibria are involved, one between the acetate released from **I** and those of HOAc and the second between complex **I** and the relevant cationic complex I^+ . The time scales of these two equilibria are not the same. Acido-basic equilibria are usually fast. The equilibrium between **I** and I^+ in eq 1 was slower, as evidenced by the detection of the protons of their respective *p*-cymene ligands. (b) The equilibrium constant in eq 1 is $K_1 = ([\text{I}^+][\text{AcO}^-])/[\text{I}]$. For each value of *n* (5, 10, 15, and 20 equiv of HOAc), the relationship is $K_1 = ([\text{I}^+]_n/[\text{I}]_n)/([\text{I}^+]_n - (nK_{\text{a}}K_{\text{HOAc}})^{1/2})$, where $[\text{I}]_n$ and $[\text{I}^+]_n$ are the concentrations of **I** and I^+ , respectively, in the presence of *n* equivalents of HOAc, with a $\text{p}K_{\text{a}}$ of 23.51 for HOAc in acetonitrile (S).^{11c} (c) Kütt, A.; Leito, I.; Kaljurand, I.; Sooväli, L.; Vlasov, V. M.; Yagupolskii, L. M.; Koppel, I. A. *J. Org. Chem.* **2006**, *71*, 2829–2838. (d) It is important to note that the ^1H NMR signals of 2-PhPy were not affected by addition of HOAc (from 1 to 5 equiv), establishing that its protonation did not occur competitively under our experimental conditions.

(12) The ^1H NMR signals of complex **I** were no longer observed after addition of 2 equiv of the stronger trifluoroacetic acid (TFA). The release of two free molecules of HOAc at 2.0 ppm (Figure S13a of the Supporting Information) was observed, together with a new complex whose *p*-cymene ligand exhibited ^1H NMR signals located downfield with respect to those of **I** (Figure S13a of the Supporting Information). This suggests the formation of either $\text{Ru}(\text{OCOCF}_3)_2(p\text{-cymene})$ by substitution of the two acetate ligands of complex **I** with two trifluoroacetates or formation of the cationic $[\text{Ru}(p\text{-cymene})(\text{CH}_3\text{CN})_4]^{2+}$ complex. The latter should not be affected by the addition of excess of TFA. When a large excess of TFA was added (from 2 to 10 equiv), a downfield shift of the aromatic protons of the ligated *p*-cymene of the new complex was observed (Figure S13b of the Supporting Information), evidence of the formation of $\text{Ru}(\text{OCOCF}_3)_2(p\text{-cymene})$ whose reversible dissociation took place in the presence of TFA to give the cationic $[\text{Ru}(\text{OCOCF}_3)(p\text{-cymene})(\text{S})]^+$ in an equilibrium similar to that in eq 1, but from $\text{Ru}(\text{OCOCF}_3)_2(p\text{-cymene})$, affected by TFA. This indicates that the *a priori* nonfavored substitution of the two acetates of **I** with a less basic ligand such as CF_3CO_2^- nevertheless occurred to generate $\text{Ru}(\text{OCOCF}_3)_2(p\text{-cymene})$. Indeed, the stronger TFA acid favored the dissociation of the acetates from **I** by formation of HOAc, confirming *a posteriori* the dissociation process of eq 1.

(13) It was initially expected that 2-PhPy would coordinate first to the Ru^{II} site giving $\text{Ru}(2\text{-PhPy})(\eta^1\text{-OAc})_2(p\text{-cymene})$, followed by dissociation of one acetate. However, the dissociation of AcO^- , especially in the presence of a small amount of free HOAc, to generate $[\text{Ru}(\text{OAc})(p\text{-cymene})(\text{S})]^+$ appears to be very easy, and the latter can then trap the 2-PhPy more rapidly than $\text{Ru}(\eta^1\text{-OAc})_2(p\text{-cymene})$ from **I**.

(14) For an $\text{S}_{\text{E}}3$ mechanism, see Scheme 7 on page 177 of ref 1g.

(15) According to DFT calculations, most acetate- or carbonate-assisted C–H bond activation by deprotonation involves an intramolecular process in which the coordinated acetate or carbonate deprotonates the initial agostic M(C–H) bond, as shown by DFT studies on Pd(II) carboxylate,^{7d,e} Pd(II) carbonate,^{7b} and Ru(II) carbonate^{4a} systems.

(16) The ^1H NMR spectrum of **A** in CD_3CN was slightly shifted toward lower field with respect to that in CDCl_3 , with an inversion of H_{11} protons vis-à-vis H_4 and H_5 , which rationalizes *a posteriori* the ability of acetonitrile to favor the dissociation of the acetate ligand from complex **A**, as established in this work.

(17) The protons of the σ -ligated *o*- $\text{C}_6\text{H}_4\text{-Py}$ in complex **A'** are located at higher field than those of complex **A** because of the respective influence of the σ -ligated pivalate or acetate.

(18) The effect of pivalate ions on the kinetics of the overall reaction could not be tested because of the formation of a heterogeneous solution in the $\text{CD}_3\text{CN}/\text{CDCl}_3$ mixture (7:3) used for the kinetic studies.

(19) (a) According to Ackermann et al.,³ⁿ the C–H bond activation of 2-PhPy by $\text{Ru}(\text{OCOMes})_2(p\text{-cymene})$ is reversible (toluene, 120 °C, 18 h) as evidenced by H–D exchange. (b) For deuteration of 2-PhPy catalyzed by Ru^{II} complexes (CD_3OD , 120 °C), see ref 4l. (c) See also ref 5h for related reversibility in the rhodium(III) series.

(20) (a) Amatore, C.; Jutand, A. *J. Organomet. Chem.* **1999**, *576*, 254–278. (b) Kozuch, S.; Amatore, C.; Jutand, A.; Shaik, S. *Organometallics* **2005**, *24*, 2319–2330.

(21) (a) Boele, M. D. K.; van Strijdonck, G. P. F.; de Vries, A. H. M.; Kamer, P. C. J.; de Vries, J. G.; van Leeuwen, P. W. N. M. *J. Am. Chem. Soc.* **2002**, *124*, 1586–1587. (b) Neufeldt, S. R.; Sanford, M. S. *Org. Lett.* **2010**, *12*, 532–535. (c) Wang, G.-W.; Yuan, T.-T.; Wu, X.-L. *J. Org. Chem.* **2008**, *73*, 4717–4720. (d) Yang, L.; Zhao, L.; Li, C.-J. *Chem. Commun.* **2010**, *46*, 4184–4186. (e) Kitahara, M.; Umeda, N.; Hirano, K.; Satoh, T.; Miura, M. *J. Am. Chem. Soc.* **2011**, *133*, 2160–2162.